

# **Typhoon parameter sensitivity of storm surge in the semi-enclosed Tokyo Bay**

Md. Rezuhanul Islam\*, Hiroshi Takagi

School of Environment and Society, Tokyo Institute of Technology, Tokyo, Japan, 152-8550

\*Corresponding author: Md. Rezuhanul Islam ([islam.m.ac@m.titech.ac.jp](mailto:islam.m.ac@m.titech.ac.jp))

## **Abstract**

In this study, a storm surge model of the semi-enclosed Tokyo Bay was constructed to investigate its hydrodynamic response to major typhoon parameters such as the point of landfall, approach angle, forward speed, size, and intensity. The typhoon simulation was validated for Typhoon Lan in 2017, and 31 hypothetical storm surge scenarios were generated to establish the sensitivity of peak surge height to the variation in typhoon parameters. The maximum storm surge height in the upper bay adjacent to the Tokyo Metropolitan Area was found to be highly sensitive to the forward speed and size of the passing typhoon. However, the importance of these parameters in disaster risk reduction has largely been overlooked by researchers and disaster managers. It was also determined that of the many hypothetical typhoon tracks evaluated, the slow passage of a large and intense typhoon transiting parallel to the longitudinal axis of Tokyo Bay making landfall 25 km southwest is most likely to cause a hazardous storm surge scenario in the upper-bay area. The results of this study are expected to be useful to disaster managers in better preparing against destructive storm surges.

**Keywords:** storm surge, risk, semi-enclosed bay, typhoon parameters, parametric study, Typhoon Lan

## **1 Introduction**

Typhoon-induced storm surges are a considerable threat to coastal inhabitants in Japan. On average, three typhoons a year make landfall on the main islands of Japan. Although the associated human losses are not extreme, with annual total fatalities of less than 40 over the past decade, billions of dollars in damage is inflicted upon Japan's infrastructure every year by these events [1,2]. In particular, the Northwest Pacific typhoon seasons of 2004, 2005, 2017, 2018, and 2019 were the most disastrous for Japan in recent decades with the occurrence of several historic typhoons, including Chaba (2004), Nabi (2005), Lan (2017), Jebi (2018), Faxai (2019), and Hagibis (2019) [2]. In 2004, more than 30,000 houses were flooded by storm surges induced by Typhoon Chaba (2004) in western Japan's Seto Inland Sea [3]. More recently, the two prosperous economic regions of Kanto and Kansai suffered their highest recorded storm surges during the passage of Typhoon Lan and Typhoon Jebi, respectively [4,5]. In 2019, the compact but strong Typhoon Faxai generated historically high waves and resultant overtopping disasters inside Tokyo Bay, causing the destruction of nearly 400 factories in Yokohama Port [6].

Precise and timely forecasts informing effective warnings are essential to mitigate the risks to life and property posed by typhoons and their associated storm surges [7,8]. The Japan Meteorological Agency (JMA) has been responsible for monitoring and reporting weather data as well as forecasting storm surge over many years. The JMA uses a two-dimensional numerical model that was improved in 2007 by incorporating a non-hydrostatic mesoscale model. The JMA model predicts multiple storm surge scenarios using different meteorological forcing fields that account for strong shoreward winds and pressure systems to consider the uncertainty in typhoon track forecasts [3]. However, one of the major shortcomings of this model is its inability to account for other variable typhoon parameters (e.g., size and forward speed) that have direct influence on storm surge generation [9]. Further improvement in storm surge forecasting is fundamental to achieving reductions in related loss of life and property

damage. Essentially, such improvement can only be achieved through in-depth understanding of both the physical parameters of storm surge as well as its behavior in a particular coastal region.

Several recent studies have attempted to use computational modeling to quantify the factors that most influence storm surge behavior. For example, Irish et al. [10] showed that storm surge tends to increase with hurricane size, and concluded that hurricane approach angle could also affect surge height. Specifically, hurricanes making landfall on the Gulf Coast of the United States with a more easterly heading were found to produce higher surges than those with a northerly track. Regarding the effect of hurricane forward speed on storm surge, an investigation of the Louisiana–Texas coasts (USA) by Rego and Li [11] revealed that slower hurricanes (with a forward speed of 12.6–18.0 km/h) cause more extensive flooding, while faster hurricanes produce higher surges but with comparatively less flood volume. Zhang and Li [12] performed an idealized numerical experiment and found that faster hurricanes increase the height of storm surge as the forced storm surge waves overlap with the Kelvin wave which cannot be seen if hurricanes move slowly. More recently, Sebastian et al. [13] found that storm surge behavior in a small water basin such as Galveston Bay (USA) is highly sensitive to the local wind direction associated with hurricane landfall location. This finding supports the conclusion of Weisberg and Zheng [14] that the greatest storm surge event would occur in Tampa Bay (USA) when a hurricane makes landfall to the north of the bay, as this would result in the occurrence of maximum winds at the mouth of the bay. Inspired by these previous numerical studies of the dependence of storm surge on the various parameters of tropical cyclones that have advanced the understanding of the storm surge climatology of the Gulf Coast of the United States, the present study examined the potential storm surge risk in Tokyo Bay, Japan.

Tokyo Bay is the most populous coastal region in the world. The population of the Tokyo Metropolis is estimated to be 13.7 million (as of May 2017) [15]. The metropolitan area is located in the innermost part of Tokyo Bay centered at 35°41'N, 139°41'E. Tokyo Bay (Fig. 1) has an intricate coastline that can either defend the megacity comprising Tokyo, Kanagawa, and Chiba Prefectures against storm

surge or render it particularly vulnerable because of trapping and amplification effects [16]. Although Tokyo is prone to the effects of typhoons, the frequency of typhoon landfall in the region is not remarkably high compared with that in southwestern Japan. Nevertheless, strong typhoons do sometimes venture into the bay. Among the major typhoons that have directly affected Tokyo Bay over the past century, a 1917 typhoon, known locally as Typhoon Taisho, was the most devastating. The storm surge induced by this typhoon claimed 1,301 lives, destroyed 43,083 houses, and swept away 8,220 marine vessels [17]. Although this represents the worst typhoon-related disaster to have affected Tokyo Bay, the mechanism of this event remains poorly understood. More recently, Typhoon Lan (2017), which was equivalent to a Category 1 hurricane at landfall, caused a 1.2-m storm surge that led to the partial inundation of the inner-bay area [4].

The large size and fast forward speed of Typhoon Lan raised concerns over whether the urban waterfronts of Tokyo and its neighboring cities are sufficiently resilient against future powerful typhoons [4]. The potential hazards in the Tokyo Bay area associated with the occurrence of a catastrophic typhoon have tended to be overlooked, possibly because such significant disasters occur infrequently. A storm surge risk assessment by the Japanese government and several recent scientific studies on Tokyo Bay have highlighted the dependence of storm surge on wind intensity, typhoon track, and sea level rise due to climate change [18–20]. However, to the best of our knowledge, the sensitivity of storm surge to the forward speed and size of typhoons has not been sufficiently investigated in this region. Better understanding of how a storm surge event might evolve in Tokyo Bay in response to all typhoon parameters is necessary to ensure robust emergency preparedness. The present study was therefore conducted to examine the sensitivity of storm surge behavior in Tokyo Bay to major typhoon parameters (i.e., landfall location, approach angle, forward speed, size, and intensity) in order to estimate the potential maximum storm surge height.

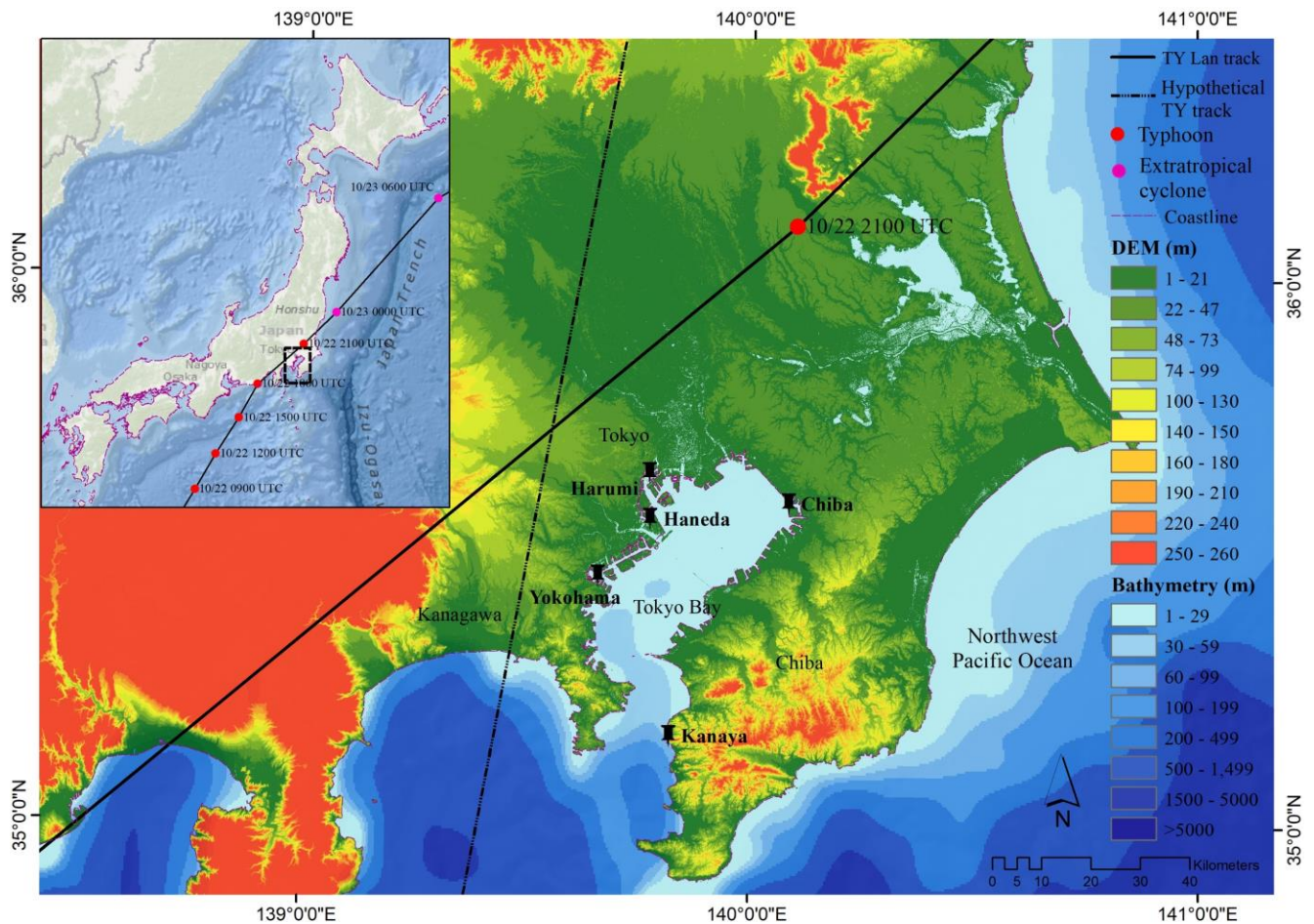


**Fig. 1** Track of Typhoon Lan (2017) as it approached the shallow coastal areas of Tokyo Bay. The black place markers indicate measurement stations used in this study (Tide: Harumi, Yokohama, Chiba and Kanaya; Wind: Haneda). The hypothetical typhoon track is described in Section 3.5 [21–24].

## 2 Methodology

### 2.1 Model description and experimental design

In this study, a series of numerical sensitivity experiments was conducted considering Typhoon Lan (2017) as the reference typhoon. Numerical simulations were performed to elucidate the influence of storm parameters (i.e., landfall location, approach angle, forward speed, storm size, and wind intensity) on storm surge generation in Tokyo Bay. For this purpose, a parametric typhoon model developed by Takagi et al. [25–28] was coupled with the Delft3D-FLOW fluid dynamics model [29]. The accuracy of this typhoon model has been validated for recent typhoons such as Haiyan (2013) [28], Goni (2015)

[30], Hato (2017) [7], and Jebi (2018) [5], all of which occurred in the Northwest Pacific basin. The typhoon model calculates both the pressure and wind fields using parameters obtained from the JMA best-track dataset, which includes the central position of the typhoon, pressure, and 50-kt (26-m/s) wind radius ( $R_{50}$ ) for each recording period. Delft3D-FLOW was then used to simulate the propagation of storm surge from the deep sea into shallow waters. As this study used a 2D horizontal grid to model the storm surge, the code is equivalent to a nonlinear longwave model as is commonly used for storm surge studies. The simulation was performed over a wide area with a grid size of 50 m (Fig. 1) that encompassed parts of Tokyo, Kanagawa, and Chiba Prefectures to assess potentially affected areas. The domain incorporated both the geometries of landfills and rivers surrounding inner Tokyo Bay, where the mean bathymetry is approximately 5 m. The bathymetry data (50-m resolution) over the target area and astronomical tide data were obtained from the Japan Coast Guard and the TPXO7.1 Global Tide Model [31], respectively. The numerical settings used in this study are listed in Table 1.

At 18:00 UTC on September 22, 2017, Typhoon Lan made landfall approximately 125 km southwest of Tokyo Bay (Fig. 1) as a strong typhoon with maximum wind speed 40 m/s (equivalent to a Category 1 hurricane on the Saffir-Simpson hurricane wind scale). Typhoon Lan was a fast-moving typhoon with a forward speed of 65 km/h at landfall and a large wind field (a 26-m/s wind radius of 389 km) that generated the highest storm tide (coinciding with rising tide) on record in Yokohama and other coastal areas (e.g., Mera in southern Chiba Prefecture) [32]. Five experimental groups (A–E) containing a total of 31 numerical conditions, detailed in Table 2, were evaluated in this study to investigate the sensitivity of surge behavior to storm parameters. The sensitivity analyses were performed by varying one of four typhoon parameters: (A) track (approach angle and landfall location), (B) forward speed, (C) size, and (D) intensity. Observations from four tide measurement stations were chosen to characterize the hydrodynamic behavior of the bay. These stations are located in the upper bay (i.e., Harumi and Chiba), middle bay (i.e., Yokohama), and lower bay (i.e., Kanaya), as shown in Fig. 1.

**Table 1** Numerical model settings for typhoon and storm surge simulation

Typhoon parameters	Typhoon Lan [23]: approach angle 140°, forward speed 65 km/h (very fast), $R_{\max}$ of 89 km (very large)
Typhoon model	Pressure: empirical estimation by Myers formula; Wind: gradient winds considering super-gradient wind effect [33]
Fluid dynamics model	Delft3D-FLOW ver. 6.02
Domain	Spherical coordinate system, grid size: 50-m mesh
Bathymetry	50-m grid spacing

To ascertain the relationship among typhoon approach angle ( $\theta$ ), landfall location, and storm surge, 21 simulations of the typhoon were performed in Group A by varying  $\theta$  from 0° to 180°, shifting its landfall location from the original landfall location of Typhoon Lan to positions 100 km to the east (approximately 25 km west of the central axis of the bay) and 150 km to the east (approximately 25 km east of the central axis of the bay), and holding all other parameters constant. In this study, the approach angle  $\theta$  is defined as the angle in degrees between the coastline and typhoon track, as measured clockwise from the coastline to the right of the landfall point when facing north. In order to investigate the extent to which typhoon forward speed influences storm surge magnitude and considering that Lan was a fast-moving typhoon, in Group B the forward speed of the typhoon at landfall was reduced to 36 and 18 km/h (two cases). These speeds are representative of the previous two major typhoons (Danas (2001) and Roke (2011)) to hit Tokyo Bay [24]. The Group C experiments focused on the effect of the maximum wind radius ( $R_{\max}$ ), used to represent the size of the strongest part of a typhoon. Because  $R_{\max}$  is not included in the JMA best-track dataset [34], we converted  $R_{50}$  data into  $R_{\max}$  using the simplified equation  $R_{\max} = 0.23 \times R_{50}$  [30]. Consequently,  $R_{\max}$  radii in the 13–89 km range at landfall time were derived for five previous major typhoons including Typhoon Lan (13 km for Danas (2001), 26 km for Mawar (2005), 43 km for Higos (2002), 55 km for Kirogi (2000), and 89 km for Lan (2017)) and used to evaluate the corresponding storm surge sensitivity (four

cases). In Group D, two wind speed cases were simulated in which the original wind speed of Lan was increased and decreased by 50%.

**Table 2** Experimental conditions, hypothesized based on Typhoon Lan (2017) as the reference typhoon.

Group	Experiment	Remarks
A	Sensitivity to typhoon track (21 cases)	Original Lan track, varied approach angle from 0° (A-1) to 180° (A-7) in 30° increments. Shifted original Lan track 100 km eastward, varied approach angle from 0° (A-8) to 180° (A-14) in 30° increments. Shifted original Lan track 150 km eastward, varied approach angle from 0° (A-15) to 180° (A-21) in 30° increments.
B	Sensitivity to typhoon forward speed (two cases)	Reduced forward speed to 36 km/h (by 45%, intermediate) (B-1) and 18 km/h (by 72%, very slow) (B-2).
C	Sensitivity to typhoon size (four cases)	Reduced $R_{\max}$ to 55 (C-1), 43 (C-2), 26 (C-3), and 13 km (very small; C-4).
D	Sensitivity to typhoon intensity (two cases)	Decreased (D-1) and increased (D-2) original Lan intensity by 50%.
E	Estimating possible maximum storm surge height (two cases)	Landfall location: 25 km southwest of Tokyo Bay, $\theta = 100^\circ$ , forward speed of 18 km/h, $R_{\max} = 89$ km, Lan intensity increased by 50% at rising (E-1) and at falling tide periods (E-2).

Finally, the experimental conditions having the greatest influence on storm surge generation in Tokyo Bay were accounted for in the estimation of a plausible maximum storm surge height (Group E in Table 2). The generation of a storm surge against a rising and falling tide can be considerably different because of interaction mechanisms between tidal current and storm current [35–36]. To address the role of tide on peak surge generation, the estimation of plausible maximum storm surge height was

carried out both (two cases) at rising (Typhoon Lan landfall time) and at falling tide periods. Semidiurnal tidal constituents dominate in Tokyo Bay. Hence, Typhoon Lan landfall time was shifted to six hours earlier (12:00 UTC on September 22, 2017) to reproduce the typhoon at falling tide periods. This landfall time is representative of the passage of a storm surge against a falling tide. The estimated storm surge height was then compared to the water levels recorded during the passage of Typhoon Lan and the worst-case scenario assumed by the Japanese government [18]. Note that in this study, the impact of waves was neglected to focus only on storm surge and to simplify the analysis.

## 2.2 Model validation

To validate the typhoon and storm surge model, simulation results using the parameters of Typhoon Lan (2017) were compared with actual data from the observation stations collected during the passage of that typhoon. A comparison of the modeled and measured wind speed [37] before and after the peak storm period at the Haneda observation station is shown in Fig. 2(a). The coefficient of determination ( $R^2 = 0.75$ ) indicates satisfactory agreement between the simulated and measured wind speed. However, the simulation error increased after the typhoon made landfall (Fig. 2(b)) as its rapid forward

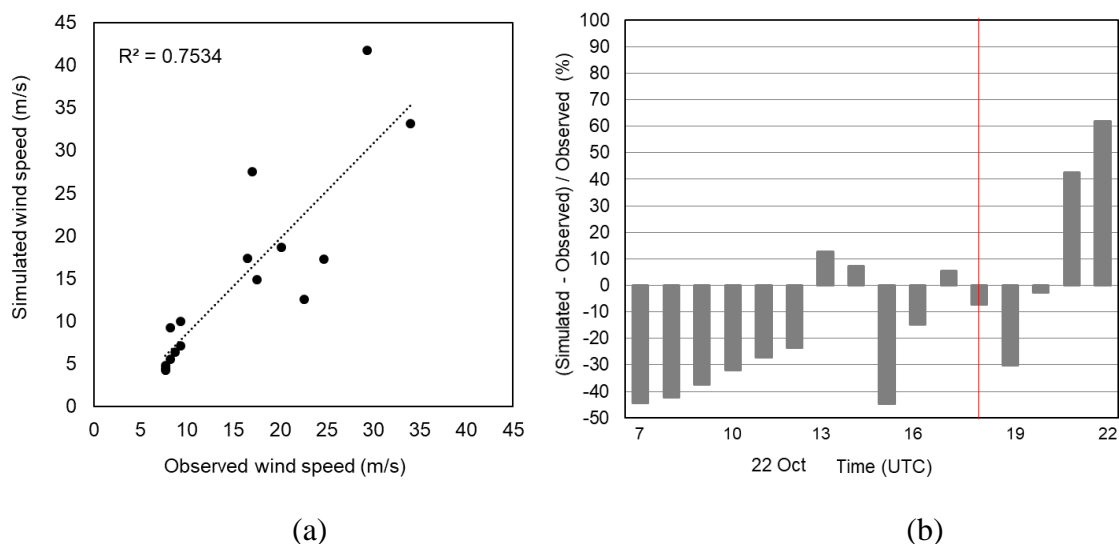
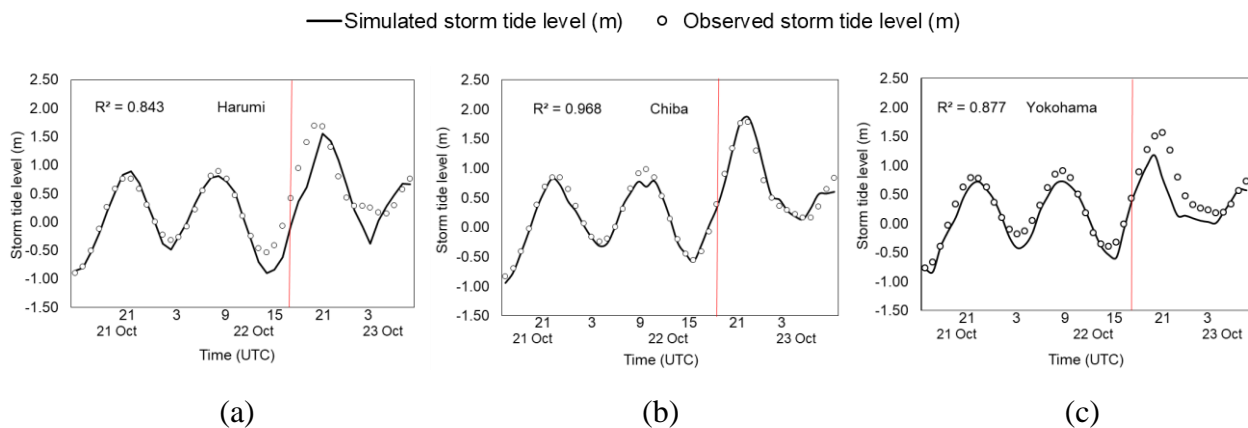


Fig. 2 (a) Simulated vs. observed wind speed at Haneda, Tokyo, and (b) estimated wind speed error ( $((\text{simulated} - \text{observed})/\text{observed wind speed} \times 100)$ ). The red vertical line indicates the time of landfall of Typhoon Lan (2017).

speed caused an abrupt change in wind speed that reduced the accuracy of the hindcast. Indeed, Typhoon Lan was a fast-moving typhoon and as such it departed the computational domain quickly after landfall.

A comparison of the simulated and measured storm tide [32] at three tide stations (Harumi, Chiba, and Yokohama) located within the computational domain is shown in Fig. 3. Model validation could not be undertaken for Kanaya because the observed storm tide data during the passage of Typhoon Lan are not available for that site. The average  $R^2$  and root mean square errors of the three stations are 0.90 and 0.21 m, respectively. Overall, the simulated water levels agree well with the recorded tide data, although the simulated peak water levels at the Harumi and Yokohama stations are slightly underestimated.



**Fig. 3** Comparison of observed and simulated storm tide at (a) Harumi, (b) Chiba, and (c) Yokohama. The red vertical lines indicate the time of landfall of Typhoon Lan (2017).

### 3 Results

#### 3.1 Sensitivity to typhoon track (Group A)

The simulation results indicated that typhoons traveling parallel ( $90^\circ \leq \theta \leq 130^\circ$ ) to the axis of Tokyo Bay tended to produce higher water levels in the upper-bay area than typhoons with a more westerly ( $150^\circ \leq \theta \leq 180^\circ$ ) or more easterly ( $0^\circ \leq \theta \leq 30^\circ$ ) heading. In contrast, the coasts adjacent to the mouth of the bay (i.e., Kanaya) tended to be more vulnerable when typhoons traversed at a more westerly

( $150^\circ \leq \theta \leq 180^\circ$ ) heading. Furthermore, typhoons traversing a more easterly ( $0^\circ \leq \theta \leq 30^\circ$ ) heading tended to cause an initial sea level drawdown of at least 1 m and dramatically steepened the storm tide profile at Yokohama. The drawdown was generated by strong, northerly offshore winds that initially drove the water southward out of Tokyo Bay. Similar sea level drawdowns or negative storm surges have also been reported for the case of San Pedro Bay of the Philippines during Typhoon Haiyan in 2013 which resulted in high velocity coastal flooding to heights of more than 7 m [38]. The results of typhoon approach angle sensitivity tests indicate that tracks more perpendicular to the coastline to the west of Tokyo Bay tend to result in predicted peak water levels 5.5% higher on average than those produced by more oblique approach angles, particularly in the upper-bay areas (i.e., Harumi and Chiba).

The center of Typhoon Lan passed approximately 125 km southwest of Tokyo Bay at a  $\theta$  of  $140^\circ$ . Figure 4(b) shows that shifting the original landfall (OL) point 100 km to the east and changing the  $\theta$  to  $90^\circ$  (Case A-11 in Table 2) increased the water level in the inner bay compared to the observed level under the original track (Fig. 4(a)). ~50% in the strong southerly wind ( $\geq 25$  m/s) blowing over the bay

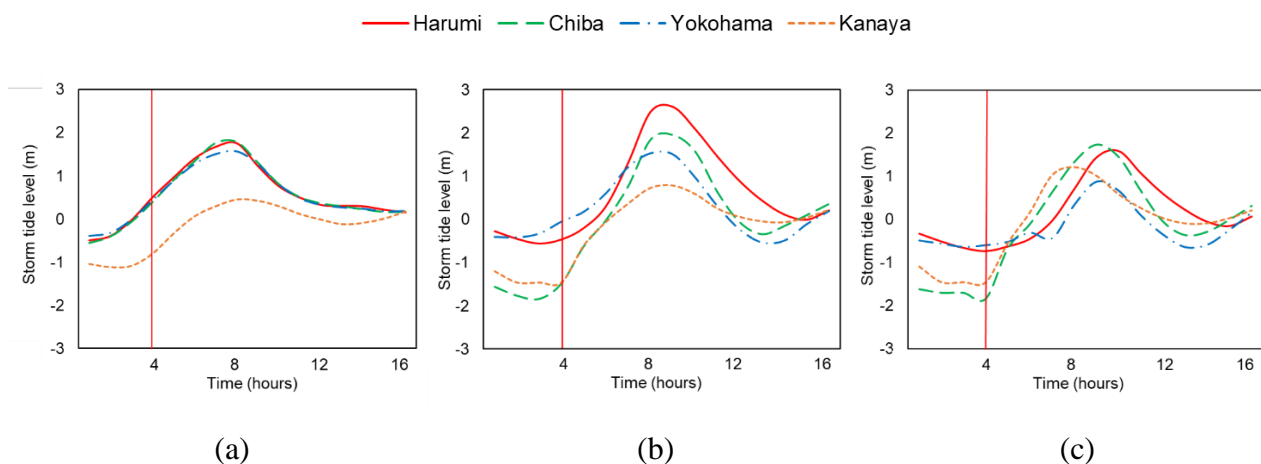


**Fig. 4** Comparison of storm tide level for selected sets of landfall locations and approach angles: (a) original landfall (OL;  $140^\circ$  approach angle), (b) 100 km east of OL and  $90^\circ$  approach angle (Case A-11), and (c) 150 km east of OL and  $90^\circ$  approach angle (Case A-18). The red vertical lines indicate time of typhoon landfall.

area due to the shift in track led to water levels 49% higher under Case A-11 than under the OL in the innermost part of the bay (i.e., Harumi). Prior to landfall, under Case A-11, easterly winds caused a buildup of water on the west coast (Yokohama) and a draw-down in the northeastern end of the bay (Chiba). Moreover, a large sea level gradient between the upper and lower ends of the bay was evident during the period of peak storm tide under Case A-11. For example, while the sea level at Harumi rose to over 2.5 m, the storm tide height at Kanaya changed from  $-1.5$  to  $0.8$  m. A similar sea level gradient, though of a smaller magnitude, was also observed during the actual Typhoon Lan event.

When the typhoon landfall was shifted 150 km to the east of the OL with an approach angle of  $90^\circ$  (Case A-18 in Table 2), the surface winds over the bay tended to be weaker than under the other evaluated tracks. However, as the typhoon tracked directly across the mouth of the bay (i.e., near Kanaya), the water levels increased by 0.8 m at Kanaya (Fig. 4(c)) relative to the OL (Fig. 4(a)). After the typhoon made landfall under Case A-18, strong northerly winds pushed the water out of the upper-bay area, while the destructive right-side semicircle of the typhoon covered the remainder of the bay. Indeed, the simulated peak storm tides for Case A-18 were slightly lower than for the OL at the upper-bay locations. In the middle of the bay (i.e., Yokohama), the dominant wind direction became westerly after landfall, resulting in comparatively lower water levels there as well. The arrival of the peak storm tide in both the upper and middle parts of the bay was delayed because the strong northward wind began to influence the water a few hours later than during the actual Typhoon Lan event.

The change in water level under different typhoon tracks confirms that the asymmetry of the wind field is highly related to the change in track. For example, the normalized frequency distribution of wind speed during landfall for Case A-11 showed that 25% of the damaging winds ( $\geq 25$  m/s) blew directly from offshore areas to the upper bay (Fig. 5(a)); however, there was almost no damaging wind in this direction when  $\theta$  was  $150^\circ$  (Case A-13) (Fig. 5(b)). These results suggest that passage of a typhoon directly over Tokyo Bay would not necessarily correspond to a more intense storm surge. However,

the upper-bay areas are clearly more vulnerable to intense storm surge under a typhoon transiting parallel to Tokyo Bay 25 km south-west of its central axis.

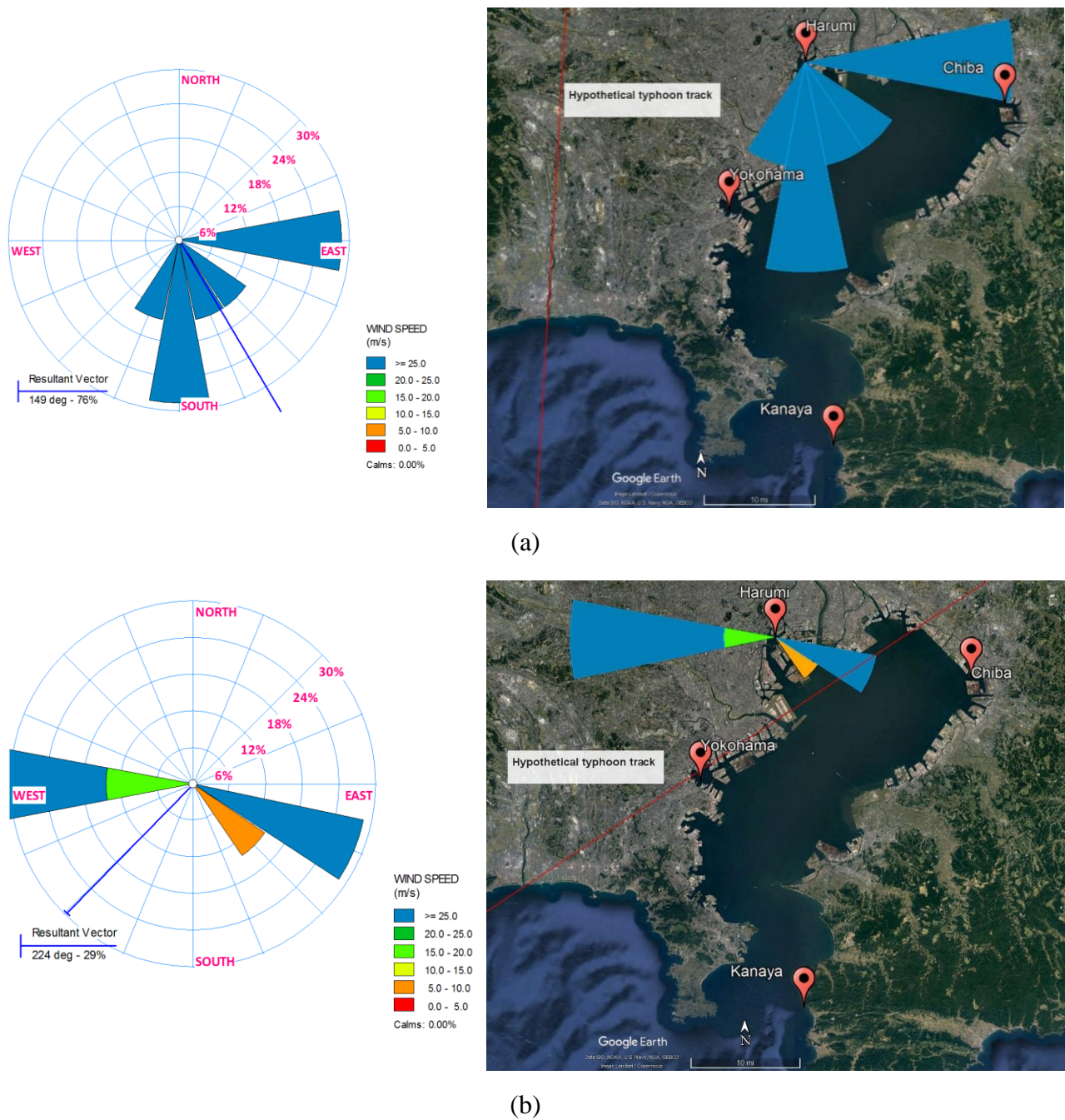


**Fig. 5** Simulated wind rose diagram at landfall for the Harumi observation station during passage of typhoon (a) Case A-11 (landfall location 25 km southwest of Tokyo Bay,  $\theta = 90^\circ$ ); (b) Case A-13 (landfall location 25 km southwest of Tokyo Bay,  $\theta = 150^\circ$ ).

### 3.2 Sensitivity to typhoon forward speed (Group B)

Typhoon Lan passed southwest of Tokyo Bay with a forward speed of 65 km/h. The simulation results shown in Fig. 6(a) indicate that a 45% reduction in forward speed to 36 km/h (Case B-1 in Table 2) resulted in no substantial difference in storm surge height except for at Yokohama. However, a much more significant reduction in speed to 18 km/h (Case B-2 in Table 2) translated into a near doubling (2.09 m) of the peak surge height in the innermost parts of the bay (i.e., Harumi), while a slight increase was evident in other places (i.e., Chiba and Yokohama). Storm surge involves the redistribution of a mass of seawater, generating a sea surface slope that depends largely on the duration of axially directed wind force over the bay. For Case B-2, the typhoon took approximately 6 h to transit the bay area, whereas it took only 3 h and 2 h for Case B-1 and the actual Typhoon Lan, respectively. With this longer duration, the cross-shore components of the wind stress were able to effectively transport more water to the shallow and geometrically complex estuaries than the faster storms (Case B-1 and the actual Typhoon Lan). Consequently, a large sea level gradient in surge height developed between the upper and lower bay.

During peak surge, the sea levels at Harumi and Chiba were considerably different (Fig. 6(a)) because (for the given typhoon track) the dominant wind direction forced horizontal redistribution of the water mass toward the northwestern end of the bay (Fig. 7). On the east coast of the bay mouth (i.e., Kanaya), the peak surge was similar to the original observation, even though the forward speed of the typhoon was reduced (Cases B-1 and B-2). On open coasts, the effective cross-shore areas over which the winds act are smaller. Therefore, the relative decrease in typhoon wind speed with decreasing forward speed resulted in minimal change in the simulated peak surge height in these areas.

Figure 6(b) compares the peak surge arrival times for slower-moving typhoons relative to the actual Typhoon Lan. Clearly, the forward speed of the typhoon strongly determines the arrival time of the maximum surge. For example, the peak surge under Case B-2 lagged behind the observed Lan peak

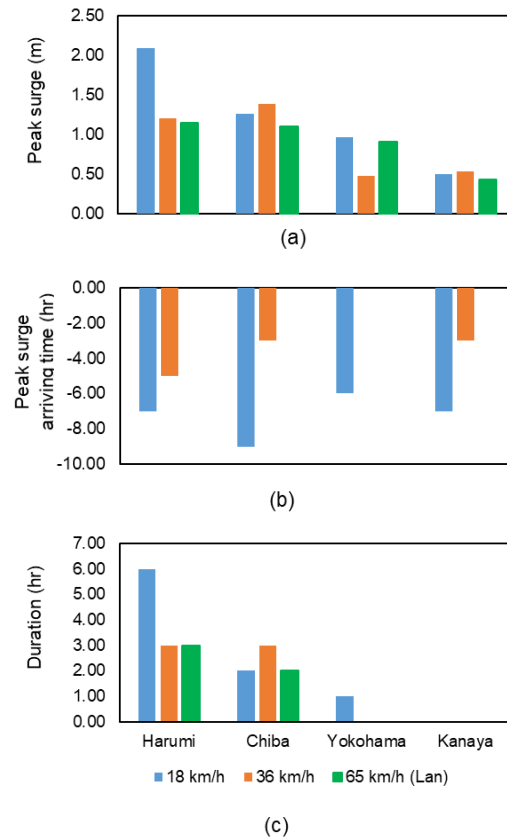


**Fig. 6** Comparison of (a) peak storm surge, (b) peak surge arrival time, and (c) duration of storm surge over 1 m for typhoons with different forward speeds. Note, the arriving times in (b) and higher surge durations in (c) are relative to those observed during the actual passage of Typhoon Lan.

by 7–9 h in the upper-bay area and by 6–7 h in the middle and lower bay. When the forward speed was double that of Case B-2 (i.e., Case B-1), the peak surge time still lagged behind the observed Lan peak by 3–5 h across the entire bay. In the simulations, both hypothetical typhoons Case B-1 and Case B-2 shifted the peak surge time to the low tide period, whereas the actual Typhoon Lan caused peak surge during the high tide period (21:00 UTC, October 22, 2017) in Tokyo Bay. This finding implies that variations in typhoon forward speed could cause the peak storm surge to coincide with low/high tide periods, which should be considered in assessing storm surge risk.

It is apparent from Fig. 6(c) that the forward speed of the typhoon also alters the duration of the highest storm surge level (i.e., over 1 m) compared with that recorded at individual stations under Typhoon

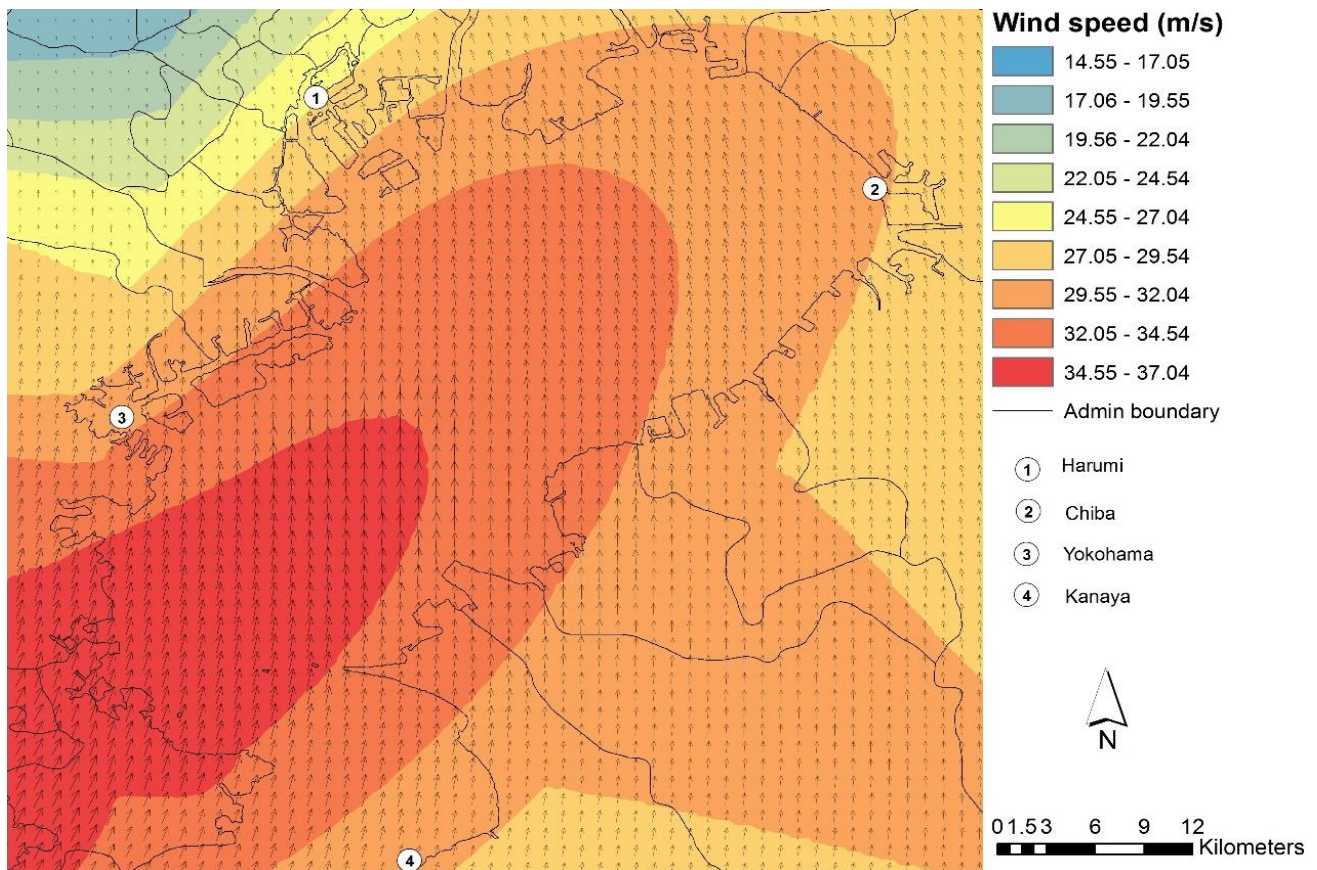


**Fig. 7** Wind speed and direction during peak surge at Harumi for typhoon forward speed of 18 km/h.

Lan. Although slowing the original forward speed to 36 km/h resulted in no substantial difference in storm surge duration, a forward speed of 18 km/h resulted in a 3-h extension of the duration of the highest storm surge level at the Harumi tidal station. In contrast, the storm surge duration at the lower-bay areas (i.e., Kanaya) remained unchanged under any typhoon speed. This is understandable because on an open coast, the buildup time is more rapid because the water is deeper, and thus the surge is less sensitive to a slow-moving typhoon. The scale of such differences between the upper and lower bay implies that the forward speed of a typhoon is an especially important parameter to consider when predicting storm surge for inner-bay locations.

### 3.3 Sensitivity to typhoon size (Group C)

Figure 8(a) illustrates the obtained relationship between typhoon size (in terms of  $R_{\max}$ ) and surge response in Tokyo Bay, indicating that storm surge height increases linearly toward the inner parts of

Tokyo Bay as typhoon size ( $R_{\max}$ ) increases. Figure 8(b) demonstrates that historical observed data support these numerical findings. Note that Chiba, Yokohama, and Kanaya are not represented in Fig. 8(b) because historical storm surge data [32] relative to mean sea level (Tokyo Peil (TP)) are not available for these sites. Furthermore, the effect of typhoon size on storm surge near open coasts (i.e., Kanaya) could not be explained properly because wave-induced buildup was neglected in the numerical model: storm size affects both the fetch and the duration of generated surface waves, so wave heights tend to increase with increasing storm size, leading to higher wave buildup and greater coastal surge along open coasts [10]. Nevertheless, the findings presented in Fig. 8(a) are consistent with the results of a storm surge study by Irish et al. [10], who demonstrated that increased storm size leads to increased storm surge, a relationship that becomes more significant over areas with a flat seabed.

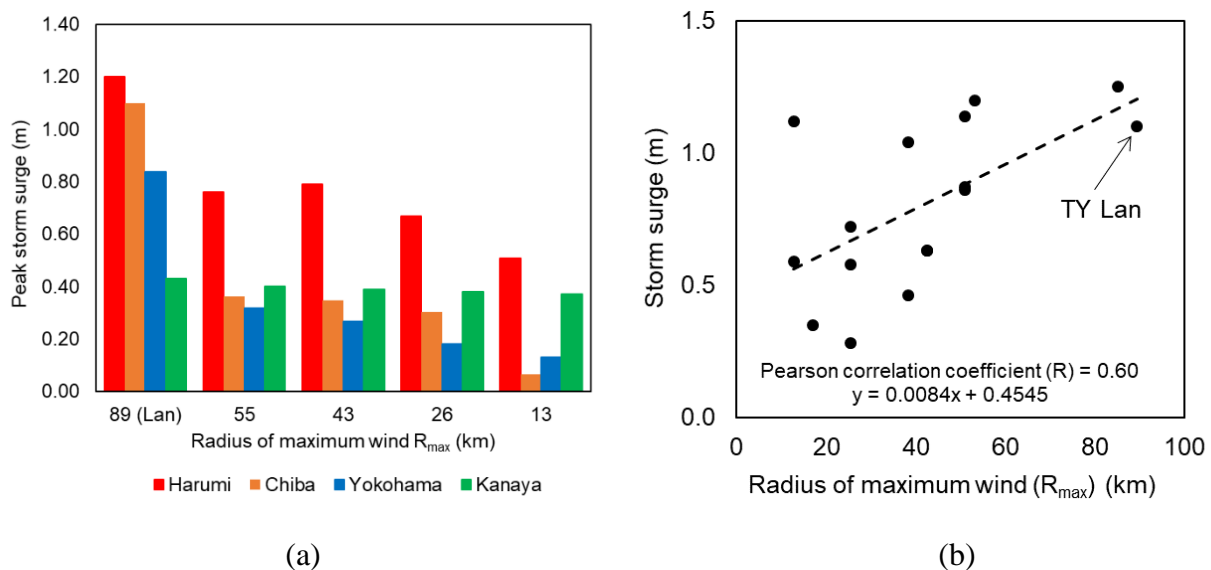


**Fig. 8** (a) Comparison of peak storm surge height (in m) for typhoons of different size (in terms of  $R_{\max}$ ) and (b) observed peak storm surge [31] vs. typhoon size ( $R_{\max}$ ) at typhoon landfall at the Harumi observation station during 1979–2018. The dashed line shows the correlation gradient between the observed storm surge and  $R_{\max}$ .

It is evident that when other typhoon parameters remain constant, the storm surge height varies with the change in typhoon size, and that this relationship is more prominent for very large typhoons. During

the approach of a large typhoon, the correspondingly large swath of strong winds affects a greater sea area and induces motion in a greater quantity of water. For example, as shown in Fig. 8(a), the observed peak surge associated with Typhoon Lan ( $R_{\max} = 89$  km) was 34% greater than that simulated for a typhoon with  $R_{\max} = 43$  km (Case C-2) in the upper-bay area (i.e., Harumi).

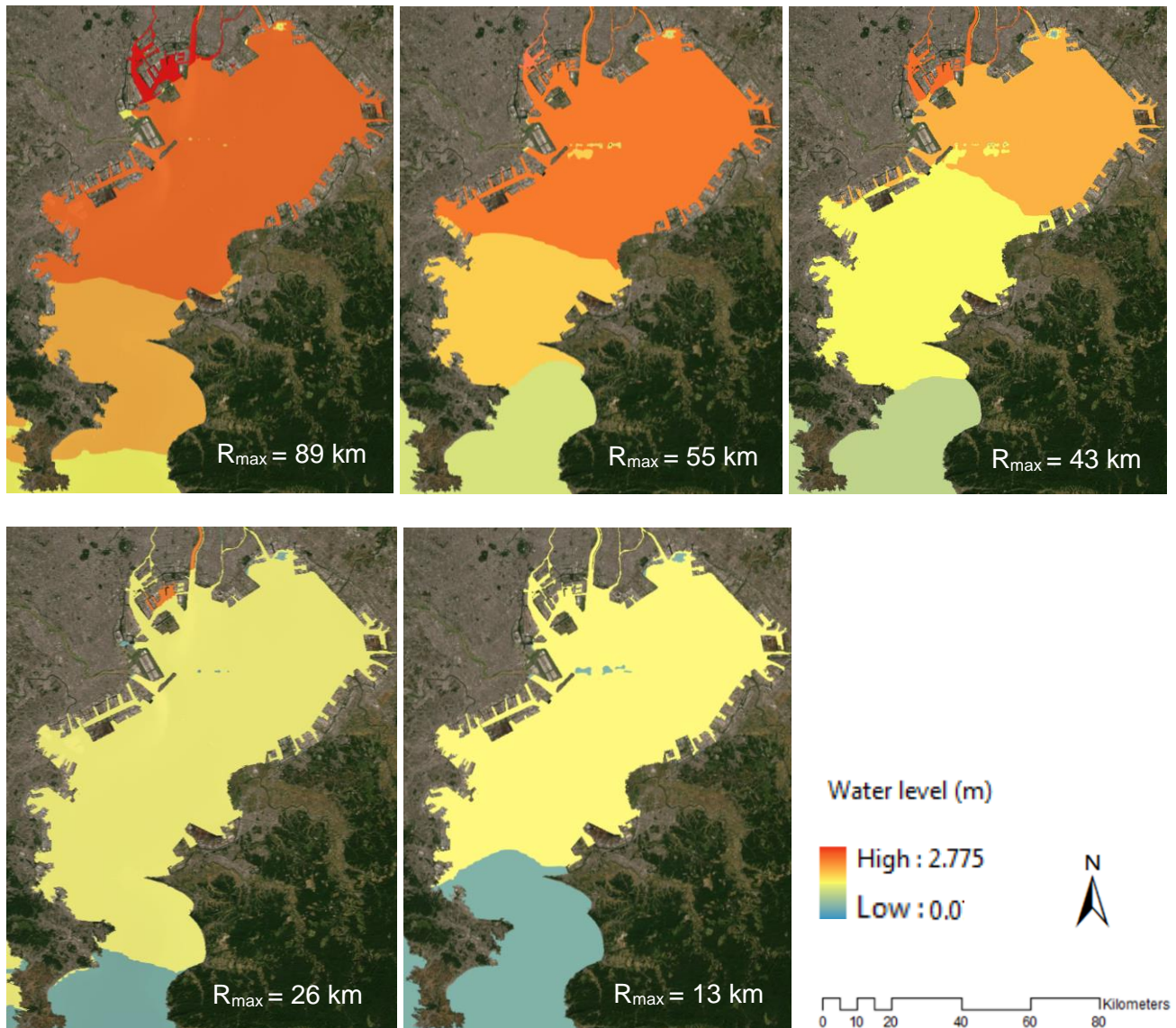


**Fig. 9** Distribution of simulated water level during the passage of Typhoon Lan over Tokyo Bay varying with  $R_{\max}$ .

It is important to note that a certain location can be affected for a longer duration by a large typhoon than a small typhoon because it takes longer for a larger typhoon to pass. Thus, it is logical that the spatial distribution of increased water level in the upper bay would also change with typhoon size, as

illustrated in Fig. 9. This finding partially explains why Typhoon Lan raised the water level by approximately 2 m in the upper areas of Tokyo Bay, even though it made landfall 125 km to the southwest. The results also show that the impact of storm surge, particularly in the inner-bay area, appears limited when a comparatively smaller typhoon (i.e., Cases C-3 and Case C-4, with  $R_{max} \leq 26$  km) passes over Tokyo Bay (Fig. 8(a)). The Group C experiments thus indicate that the passage of a typhoon far from a semi-enclosed bay would not necessarily imply the occurrence of a correspondingly small storm surge. Nevertheless, upper-bay areas are shown to be more vulnerable to intense storm surge when a typhoon with a large swath of strong winds makes landfall.

#### 3.4 Sensitivity to typhoon intensity (Group D)

Figure 10 presents comparisons of observed storm surge and numerical model output for two hypothetical typhoons in which the original wind speed of Typhoon Lan was strengthened by 50% (Case D-1) and weakened by 50% (Case D-2). Increasing the intensity of Lan (Case D-1) resulted in a 40–70% increase in storm surge height in the upper-bay area (i.e., Harumi and Chiba), whereas the

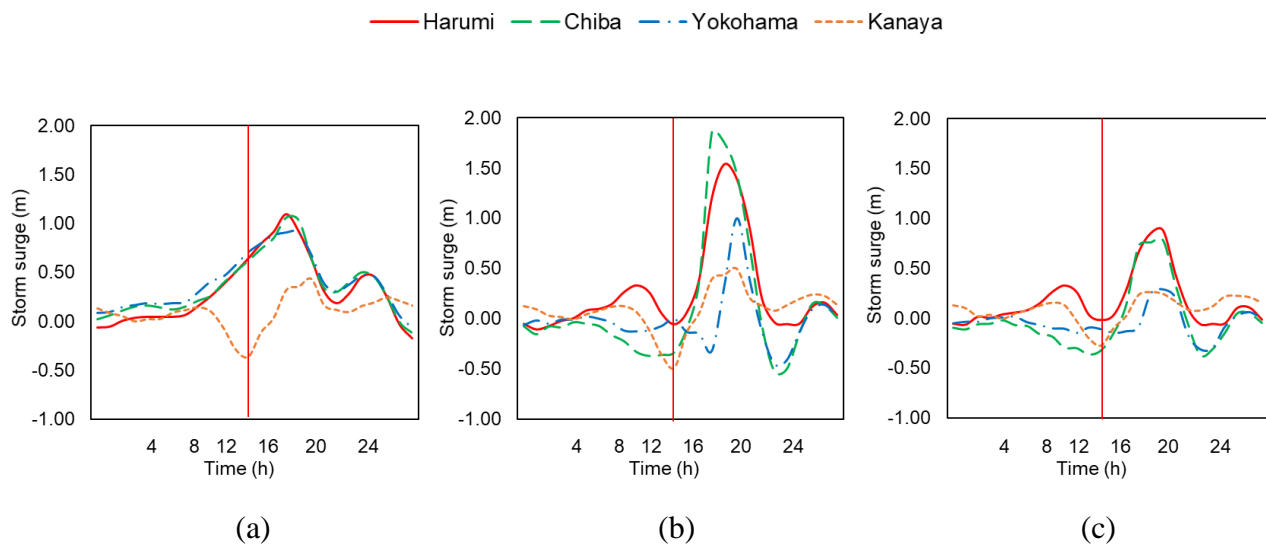


**Fig. 10** Storm surge hydrographs generated for (a) original Typhoon Lan, (b) 50% increase in Typhoon Lan wind speed, and (c) 50% decrease in Typhoon Lan wind speed. The red vertical lines indicate time of landfall.

increase was limited to 15% in the middle (i.e., Yokohama) and lower-bay areas (i.e., Kanaya). In Case D-2, although a 0.6-m difference in sea surface height existed between the upper- and lower-bay areas, a decrease in storm surge height was also evident at all stations. This sensitivity test implies that storm surge height changes exponentially in relation to surface wind speed, which is consistent with the literature (i.e. [39]). Furthermore, the surge hydrographs shown in Fig. 10 suggest that the arrival and recession time of the peak surge was reasonably constant within the bay system, i.e., little variation was found with the change in typhoon intensity. The shape of the surge hydrograph is more sensitive to typhoon track and forward speed, as discussed in relation to the results of the Group A and Group B experiments in Sections 3.1 and 3.2, respectively.

### 3.5 Estimating possible maximum storm surge height (Group E)

Figure 11(b) shows an example of the maximum storm surge height in Tokyo Bay determined by combining the experimental conditions found most influential in raising the water level (landfall location 25 km southwest of Tokyo Bay (Fig. 1),  $\theta = 100^\circ$ , forward speed of 18 km/h,  $R_{\max} = 89$  km, and Typhoon Lan wind intensity increased by 50%). This case was executed in such a manner that typhoon landfall time coincided with high tide (Typhoon Lan landfall time) (Case E-1). In the innermost part of the bay (i.e., Harumi), the storm surge height increased to 3 m (storm tide: 3.5 m) from 1.2 m (storm tide: 1.7 m) under Typhoon Lan, shown in Fig. 11(a), exceeding the government approximated maximum value of 2.5 m [18], shown in Fig. 11 (c), by 20%. Such a variation could be explained by the differences in the experimental conditions. In the government assessment of storm surge risk, a landfall location 25 km southwest of Tokyo Bay, typhoon approach angle of approximately  $100^\circ$ , forward speed of 50 km/h, and intensity of 915 hPa at landfall time, as well as a sea level rise of 0.6 m due to global warming were assumed [18]. However, the influence of typhoon size and speed, in this case a large and slow typhoon, was ignored when estimating the worst-case scenario for Tokyo Bay.

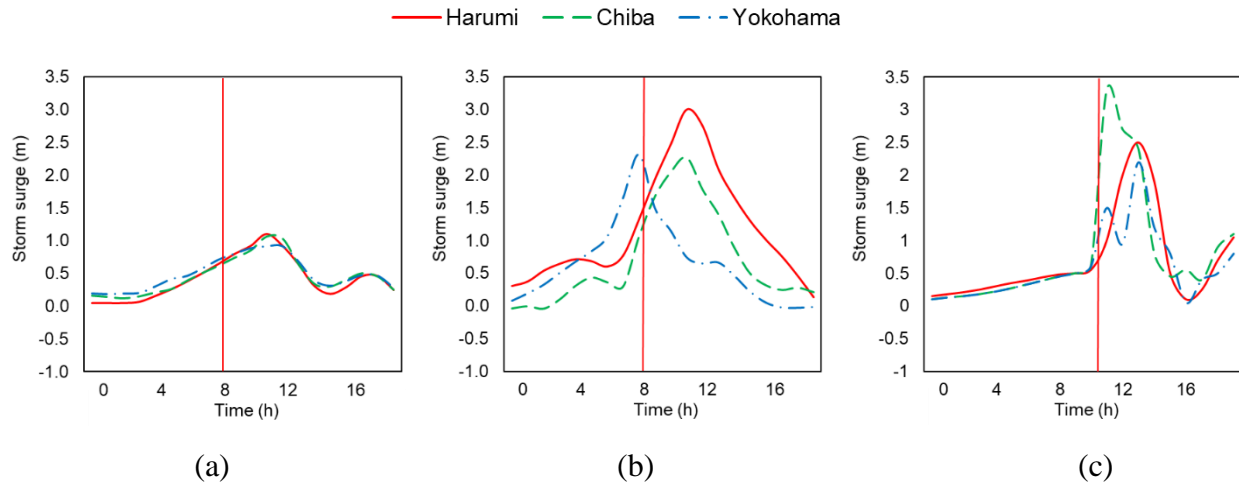


**Fig. 11** Comparison of storm surge heights due to (a) Typhoon Lan; (b) a hypothetical typhoon (landfall location 25 km southwest of Tokyo Bay,  $\theta = 100^\circ$ , forward speed of 18 km/h,  $R_{\max} = 89$  km, Lan intensity increased by 50%); and (c) the hypothetical typhoon assumed by Ministry of Land, Infrastructure, Transport and Tourism (MLIT) (landfall location 25 km southwest of Tokyo Bay,  $\theta = 100^\circ$ , forward speed of 50 km/h, intensity of 915 hPa at landfall time, sea level rise of 0.6 m due to global warming). The red vertical lines indicate time of landfall.

Estimation of the possible maximum storm surge height was also carried out at the falling tide period (Case E-2). Although the peak storm surge height in the inner most part of the bay (i.e., Harumi) remained the same (2.86 m), the maximum storm tide level (2 m) decreased by 43%. Previous literature studies [35-36] have stated that non-linear tide-surge interactions often significantly contribute to peak storm surge. However, the present study could not confirm the role of such non-linear behavior on storm surge generation because storm wave modelling was not conducted: wave can contribute to local current, bottom stress, and wave radiation stress considerably which control the non-linear tide-surge interaction [40].

The comparison of the simulated time series of storm surge height at the Harumi tidal station shown in Fig. 11(b) indicates that dangerous storm surges (i.e., over 1 m above TP) began to arise 3-h prior to the peak and took 5 h to recede below 1 m after the peak storm surge occurred, for a total duration of 9 h. In contrast, the dangerous storm surge (i.e., over 1 m above TP) event is shown to be a short

period (4 h) phenomenon by the government assessment in Fig. 11(c), mainly because of the failure to account for the effects of a large and slow-moving typhoon. Although the peak storm surge heights at the other tidal stations did not change as much as those in the innermost part of the bay, their relative changes would vary further given a different set of experimental conditions. Note that the storm surge hydrograph for Kanaya is not presented in Fig. 11 because no government assessment for this site was available. This finding suggests that surge generation in a semi-enclosed bay is dependent not only on the intensity/track of a typhoon but also on its forward speed and size, particularly in upper-bay areas.

#### **4 Discussion**

Currently, the Tokyo Metropolis accounts for 10.6% of Japan's total population and it is projected that this number could approach 12.8% by 2045 [15]. The occurrence of typhoon-induced storm surge in Tokyo Bay could therefore not only devastate local infrastructure and cause loss of life, but also has the potential to cause unprecedented national economic and environmental damage. When predicting the risk of coastal storm surges in Tokyo Bay, wind intensity and typhoon track have traditionally been evaluated as the predominant forcing factors. However, based on the example of Typhoon Lan, this study determined that the forward speed and size of a typhoon also exert substantial influence on the risk of coastal storm surges, particularly in the inner-most part of Tokyo Bay adjacent to the Tokyo Metropolitan Area. Findings based on numerical simulations in this study suggest that “a large and slow-moving intense typhoon transiting parallel to the longitudinal axis of Tokyo Bay on a track 25 km to the southwest” is more likely than a faster and smaller intense typhoon to cause hazardous storm surge in the upper-bay area. The results also indicate that the water surface elevation varies according to the intensity and track of a typhoon, consistent with current knowledge.

Typhoon forward speed is an oft-overlooked parameter in storm surge research. The present study has demonstrated that a slow-moving typhoon not only increases the peak storm surge height but also affects the peak surge arrival time and the duration of the dangerous storm surge level in the upper-

bay area. Although a slower typhoon could produce a greater storm surge in the bay, a fast-moving typhoon could be equally hazardous or generate a higher surge, especially on open coastlines as it would tend to coincide with the long wave propagation speed, which could energize shelf waves [11, 41-42]. It would appear that coastal geometry (i.e., a semi-enclosed bay or open coastline) is a critical factor in determining the relationship between storm surge and typhoon forward speed [43].

Considering forward speed to be a function of latitude, some researchers have assumed that the forward speed of a typhoon approaching Tokyo Bay (latitude: approximately 35°N) would exceed 45 km/h (i.e., [20]). Based on this assumption, the government storm surge risk assessment [18] neglected the influence of slow-moving typhoons. However, the frequency of occurrence of slow-moving typhoons is not negligible: of the 18 typhoons that made landfall between 1961 and 2019, five were found to have a forward speed of less than 25 km/h at the time of landfall [24]. Typhoon Faxai (2019), which made landfall near Tokyo Bay (Fig. 12) at a forward speed of 25 km/h, is a recent example of such slow-moving typhoons. Although its intensity was not extreme, it was still able to produce a historically high storm surge of 1.4 m in Chiba that remained above 1 m for 3 h [32]. Slow-moving Typhoon Faxai likely excited the sea state inside the bay due to its slow progression, resulting in high waves and greater storm surges that significantly damaged the port area of Yokohama. On the other hand, wind disasters were severe, and damage occurred in various places of Chiba prefecture, such as building roofs scattering and the power poles collapsing. [6]. Therefore, the combined hazards from storm surge flooding, extreme winds, and the prevailing vulnerabilities must be considered when developing appropriate evacuation strategies.

The relationship between typhoon size and storm surge height has also been underestimated partially because the JMA only began monitoring typhoon size in 1978, meaning that few examples of very large typhoons such as Lan (2017) exist in the database. The variation in many of the recorded storm surges in Tokyo Bay could indeed be explained by differences in typhoon size. Typhoon Tip (1979) is a good example of a very large typhoon, as it had an  $R_{50}$  value of 370 km, four times larger than that

of Typhoon Faxai (2019) ( $R_{50} = 93$  km) (Fig. 12). Typhoon Tip produced a storm surge 25% (1.25 m) greater than that generated by Typhoon Faxai (1 m) in the innermost part of Tokyo Bay (i.e. Harumi) [24, 32]. Regardless of Tip's fast-moving speed (75 km/h), the maximum sustained wind speed (40 m/s) and approach angle were comparable with Faxai (Table 3). It is notable that Typhoon Tip made landfall much farther away: approximately 430 km southwest of the Tokyo Bay (i.e., Minabe in Wakayama prefecture) [24] but still managed to elevate historically highest water level of 2 m in the inner Tokyo Bay (i.e. Harumi) [32]. Given the landfall location, however, the fast-moving speed might not be the major influencing factor in generating high storm surges in the case of Typhoon Tip. The greater storm surge from the larger Typhoon Tip was the result of the wider sea area affected, thus inducing motion in a greater quantity of water. The large swath of Tip's strong wind caused severe damage such that the agricultural and fishing industries sustained losses of 105.7 billion JPY [2].

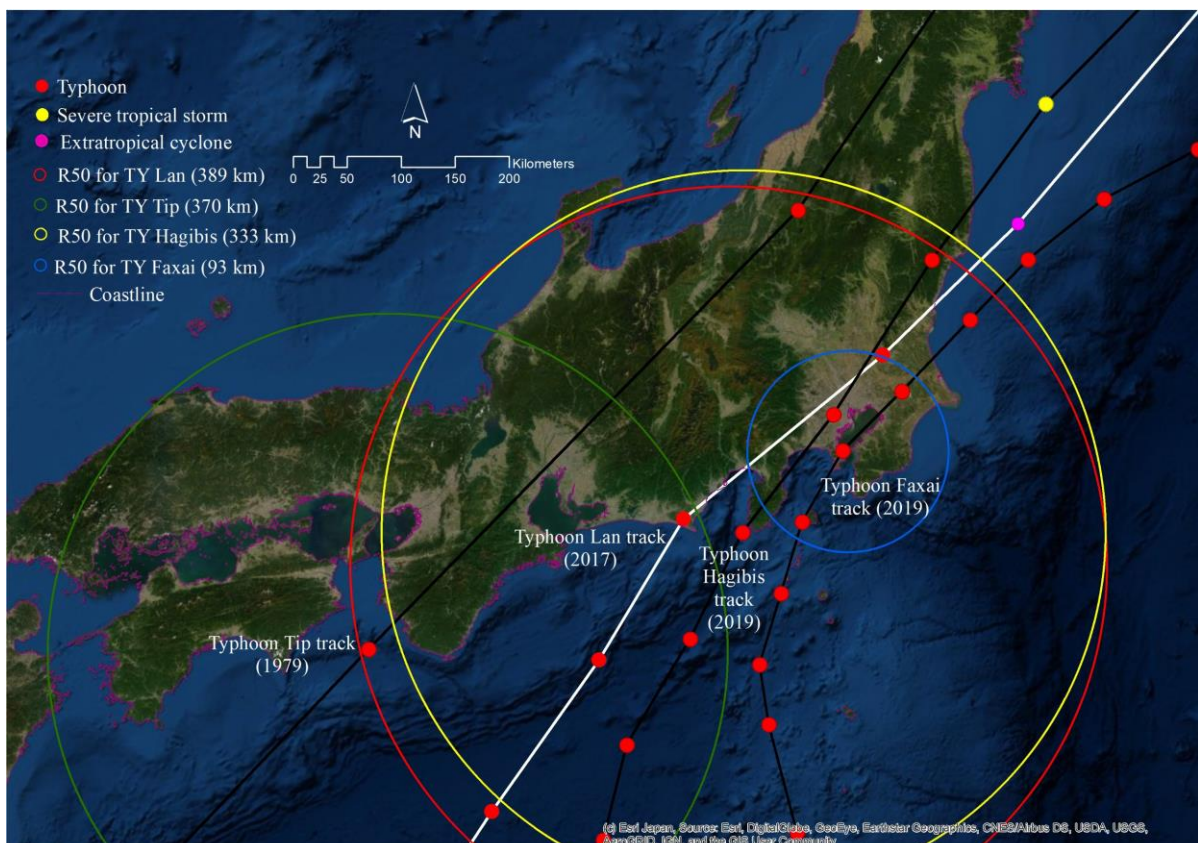


**Fig. 12** Tracks and 50 kt (26 m/s) wind radii ( $R_{50}$ ) of Typhoon Tip (1979), Typhoon Lan (2017), Typhoon Faxai (2019), and Typhoon Hagibis (2019) during their approach to Japan [24].

Estimation of possible maximum storm surge height based on a hypothetical typhoon has also informed several important lessons for future disaster risk management in Japan. Although the potential peak storm surge and inundation heights along Tokyo Bay are provided on the risk map edited by MLIT [18], it remains important to evaluate the reliability of these predicted values through comparison with other hypothetical conditions. Typhoons that caused high storm surges in Tokyo Bay mostly made landfall to the southwest ( $100 \pm 95$  km) of the central bay axis, with wind speeds of 28 to 41 m/s, an average forward speed of 46 km/h ( $\pm 19$  km/h; standard deviation), and a mean  $R_{50}$  of 230 km ( $\pm 110$  km; standard deviation) (Table 3). Considering historical typhoon tracks and intensities, MLIT [17] developed a total of six scenarios (A, B, C, D, E, and F) to estimate the expected peak storm surge height. In the worst case (Scenario F), they assumed that a fast-moving typhoon (50 km/h) with a central pressure of 915 hPa at the time of landfall (equivalent to the Muroto Typhoon (1934),

**Table 3** Top ten typhoons (1979–2009) impacting upper Tokyo Bay (i.e., Harumi) according to resultant maximum storm surge [24, 32]

Typhoon name (Year)	Peak storm surge (m)	Landfall location from central bay axis in km (direction)	Approach angle relative to coastline (degree in clockwise direction)	Forward speed at landfall (km/h)	Radius of $R_{50}$ at landfall (km)	Max. 10- min sustained wind speed at landfall (m/s)
Hagibis (2019)	1.38	50 (southwest)	130	37	333	35
Tip (1979)	1.25	430 (southwest)	135	75	370	36
Irma (1985)	1.20	80 (southwest)	130	69	232	33
Lan (2017)	1.20	125 (southwest)	140	65	389	41
Danas (2001)	1.12	over Tokyo Bay	120	24	56	28
Roke (2011)	1.14	190 (southwest)	140	46	222	41
Fitow (2007)	1.04	50 (southwest)	110	23	167	33
Faxai (2019)	1.01	over Tokyo Bay	135	24	93	41
Melor (2009)	0.87	250 (southwest)	145	58	222	36
Jelawat (2012)	0.86	230 (southwest)	130	50	222	36

and stronger than Typhoon Lan by 35 hPa) would travel parallel to Tokyo Bay on a track 25 km to the southwest (Fig. 1). They also assumed that owing to global warming, 0.6 m of sea level rise would have taken place so that in their present state, coastal defenses (i.e. sluice gates, breakwaters, and sea walls) would be damaged. These hypothetical typhoon conditions clearly excluded the combined effects of a large and slow-moving typhoon when estimating the possible maximum coastal surge in the governmental assessment. In this regard, it would be rational to re-evaluate the storm surge risk potentials for not only Tokyo Bay, but perhaps for other areas that have not considered the combined influence of size and forward speed along with other typhoon parameters. The hazardous typhoon conditions addressed in Section 3.5 of this study are only hypothetical. However, the recent Typhoon Hagibis (2019) (Fig. 12) may be considered a close approximation (Table 3) of the hypothetical case. In addition to its relatively slow-moving speed (37 km/h) compared to the historical average (46 km/h), Hagibis was categorized as a large ( $R_{50} = 333$  km) and strong (10-minute sustained wind speed of 40 m/s) typhoon that made landfall 50 km southwest of Tokyo Bay and resulted in the highest storm surge in recorded history of 1.38 m in the innermost part of Tokyo Bay [24, 32]. Assuming that typhoon parameters can be independent of each other, the likelihood that any given slow-moving typhoon transiting parallel on a track 25 km southwest of Tokyo Bay simultaneously being large and very strong can be considered small, but nonetheless quite real. Such an unusual typhoon condition clearly demonstrates its importance as an extreme hazardous scenario similar to other conventionally evaluated worst cases (i.e., the storm surge risk assessment criteria assumed by MLIT).

## **5 Conclusions**

For decades, typhoon disaster management in Japan has emphasized wind intensity and typhoon track to be the most dominant factors when predicting and issuing warnings for dangerous coastal storm surges. However, their forecasting techniques have not adequately accounted for the importance of other typhoon parameters to date. Considering the growing concern regarding the potential for

unprecedented storm surges in the present-day Tokyo metropolitan region, this study determined the most influential typhoon parameters in storm surge generation. The results obtained suggest that incorporation of typhoon forward speed and size could help meteorologists and oceanographers provide more robust surge forecasts for Tokyo Bay.

The sensitivity analyses presented in this paper demonstrate variations in storm surge heights related to principal typhoon parameters including landfall location, approach angle, forward speed, size, and intensity, focusing on Tokyo Bay; however, variations in typhoon parameters could also influence the generation of wind waves, which was not addressed in this study. Further research in this area should therefore examine the combined effects of wave setup as these factors can also influence storm surge distribution. The results of the present study are based on only one historical case (Typhoon Lan). To better support future emergency planning and risk management in the vicinity of the Tokyo Bay, an extension from current scenario-based study to a probabilistic hazard assessment study is necessary.

## **Acknowledgments**

The first author is thankful to the Ministry of Education, Culture, Sports, Science, and Technology (MEXT) of Japan for the provided scholarship to conduct research in the field of disaster risk reduction. This research was funded through the grants for Tokyo Institute of Technology (Japan Society for the Promotion of Science, 16KK0121, 19K04964, and 19K24677). Best track data for 1961–2019 (<https://www.jma.go.jp/jma/jma-eng/jma-center/rsmc-hp-pub-eg/trackarchives.html>), observed tide (<http://www.data.jma.go.jp/kaiyou/db/tide/genbo/index.php>), typhoon statistics (<https://www.data.jma.go.jp/fcd/yoho/typhoon/statistics/index.html>) and past weather (<http://www.data.jma.go.jp/obd/stats/etrn/index.php>) data were provided by the Japan Meteorological Agency. No potential conflict of interest was reported by the author(s).

## References

- [1] Japan Meteorological Agency (2019a). Typhoon statistics (in Japanese). [Available at <https://www.data.jma.go.jp/fcd/yoho/typhoon/statistics/index.html>]
- [2] Digital Typhoon (2019). Typhoon Damage List.[Available at <http://agora.ex.nii.ac.jp/cgi-bin/dt/disaster.pl?lang=en&basin=wnp&sort=damage&order=dec&stype=number>]
- [3] Higaki M, Hironori H, Nozaki, F (2009) Outline of the Storm Surge Prediction Model at the Japan Meteorological Agency. In: The Technical Review - RSMC Tokyo-Typhoon Center, 25 – 38. <https://www.jma.go.jp/jma/jma-eng/jma-center/rsmc-hp-pub-eg/techrev/text11-3.pdf>
- [4] Islam M R, Takagi H, Anh L T, Takahashi A, Bowei K (2018). 2017 Typhoon Lan Reconnaissance Field Survey in Coasts of Kanto Region, Japan. *Journal of Japan Society of Civil Engineers, Ser. B3 (Ocean Engineering)*, 74(2). [https://doi.org/10.2208/jscejoe.74.I\\_593](https://doi.org/10.2208/jscejoe.74.I_593)
- [5] Anh L T, Takagi H, Heidarzadeh M, Takata Y, Takahashi A (2019). Field Surveys and Numerical Simulation of the 2018 Typhoon Jebi: Impact of High Waves and Storm Surge in Semi-enclosed Osaka Bay, Japan. *Pure and Applied Geophysics*, 176(10): 4139 – 4160. <https://doi.org/10.1007/s00024-019-02295-0>
- [6] Takagi H, Islam M R, Anh L T, Takahashi A, Sugiu T, Furukawa F (2020). Investigation of high wave damage caused by 2019 Typhoon Faxai in Kanto region and wave hindcast in Tokyo Bay. *Journal of Japan Society of Civil Engineers, Ser. B3 (Ocean Engineering)*, 76(1). [https://doi.org/10.2208/jscejoe.76.1\\_12](https://doi.org/10.2208/jscejoe.76.1_12)
- [7] Takagi H, Xiong Y, Furukawa F (2018). Track analysis and storm surge investigation of 2017 Typhoon Hato: were the warning signals issued in Macau and Hong Kong timed appropriately? *Georisk: Assessment and Management of Risk for Engineered Systems and Geohazards*, 12: 297 –307. <https://doi.org/10.1080/17499518.2018.1465573>.
- [8] Takagi H, Xiong Y, Fan J (2019). Public Perception of Typhoon Signals and Response in Macau: Did Disaster Response Improve between the 2017 Hato and 2018 Mangkhut. *Georisk: Assessment and Management of Risk for Engineered Systems and Geohazards*. <https://doi.org/10.1080/17499518.2019.1676453>
- [9] Needham H F, Keim B D (2011). Storm surge: Physical processes and an impact scale. In: Lupo E, ed. *Recent Hurricane Research—Climate, Dynamics, and Societal Impacts*. Croatia: Intech Open Access, 386 – 394
- [10] Irish J L, Resio D T, Ratcliff J J (2008). The Influence of Storm Size on Hurricane Surge. *Journal of Physical Oceanography*, 38(9): 2003 – 2013. [doi: 10.1175/2008JPO3727.1](https://doi.org/10.1175/2008JPO3727.1).
- [11] Rego J L, Li C (2009). On the Importance of the Forward Speed of Hurricanes in Storm Surge Forecasting: A Numerical Study. *Geophysical Research Letters*, 36: L07609. <https://doi.org/10.1029/2008GL036953>.
- [12] Zhang C, Li C (2019). Effects of hurricane forward speed and approach angle on storm surges: an idealized numerical experiment. *Acta Oceanologica Sinica*, 38(7): 48 – 56. <https://doi.org/10.1007/s13131-018-1081-z>
- [13] Sebastian A G, Proft J M, Dietrich J C, Du W, Bedient P B, Dawson C N (2014). Characterizing hurricane storm surge behavior in Galveston Bay using the SWAN + ADCIRC model. *Coastal Engineering*, 88: 171 – 181. <https://doi.org/10.1016/j.coastaleng.2014.03.002>
- [14] Weisberg R H, Zheng L (2006). Hurricane storm surge simulations for Tampa Bay. *Estuaries and coasts*, 29(6): 899 – 913. <https://doi.org/10.1007/BF02798649>
- [15] Ministry of Health, Labour and Welfare (Japan) (2018). Statistics and other data. [Available at <https://www.mhlw.go.jp/english/database/index.html>]
- [16] Hirano K, Bunya S, Murakami T, Iizuka S, Nakatani T, Shimokawa S, Kawasaki K (2014). Prediction of typhoon storm surge flood in Tokyo Bay using unstructured model ADCIRC under global warming scenario. In: *Proceedings of 4th Joint US-European Fluids Engineering Division Summer Meeting and 12th International Conference on Nanochannels, Microchannels, and Minichannels*. Chicago, Illinois, USA: ASME.

- [17] Omori F (1918). Tsunami in Tokyo Bay. In: Earthquake Investigation Committee Report, 89, 19 – 48 (in Japanese).
- [18] Ministry of Land, Infrastructure and Transport (Japan) (2009). Estimation of large scale inundation scenario by storm surge at Tokyo Bay (in Japanese). [Available at [http://www.mlit.go.jp/report/press/port07\\_hh\\_000017.html](http://www.mlit.go.jp/report/press/port07_hh_000017.html).]
- [19] Hoshino S, Esteban M, Mikami T, Takagi H, Shibayama T (2015). Estimation of increase in storm surge damage due to climate change and sea level rise in the Greater Tokyo area. *Natural Hazards*, 80(1): 539 – 565. <https://doi.org/10.1007/s11069-015-1983-4>
- [20] Nakajo S, Fujiki H, Kim S, Mori N (2018). Sensitivity of tropical cyclone track to assessment of severe storm surge event at Tokyo Bay. In: Proceedings of 36<sup>th</sup> International Conference on Coastal Engineering, Baltimore, Maryland, USA. <https://doi.org/10.9753/icce.v36.papers.5>.
- [21] Japan Oceanographic Data Center (2000). 500 m Gridded Bathymetric Feature Data around Japan. [Available at [https://jdoos1.jodc.go.jp/vpage/depth500\\_file.html](https://jdoos1.jodc.go.jp/vpage/depth500_file.html).]
- [22] Japan Aerospace Exploration Agency (2015). 30 m World Elevation Data Site. [Available at <https://www.eorc.jaxa.jp/ALOS/en/aw3d30/data/index.htm>.]
- [23] Geospatial Information Authority of Japan (2016). GSI Japan Global map site. [Available at [https://www.gsi.go.jp/kankyochiri/gm\\_japan\\_e.html](https://www.gsi.go.jp/kankyochiri/gm_japan_e.html).]
- [24] Japan Meteorological Agency (2019b). Typhoon Best Track Data Site. [Available at <https://www.jma.go.jp/jma/jma-eng/jma-center/rsmc-hp-pub-eg/trackarchives.html>]
- [25] Takagi H, Thao N D, Esteban M, Tam T T, Knaepen H L, Mikami T (2012). Assessment of the coastal disaster risks in Southern Vietnam. *Journal of Japan Society of Civil Engineering*, B3 (Ocean Engineering), 68(2): 888 – 893. <http://dx.doi.org/10.2208/jscejoe.68.I.888>.
- [26] Takagi H, Thao N D, Esteban M (2014). Tropical cyclones and storm surges in Southern Vietnam. In: Thao N D, Takagi H, Esteban M, eds. *Coastal Disasters and Climate Change in Vietnam*. Elsevier: 3 – 16. <http://dx.doi.org/10.1016/B978-0-12-800007-6.00001-0>.
- [27] Takagi H, Esteban M, Shibayama T, Mikami T, Matsumaru R, Nguyen D T, Oyama T, Nakamura R (2015). Track analysis, simulation and field survey of the 2013 Typhoon Haiyan storm surge. *Journal of Flood Risk Management*, 10: 42 – 52. <http://dx.doi.org/10.1111/jfr3.12136>.
- [28] Takagi H, Li S, de Leon M, Esteban M, Mikami T, Matsumaru R, Shibayama T, Nakamura R (2016). Storm surge and evacuation in urban areas during the peak of a storm. *Coastal Engineering*, 108: 1 – 9. <https://doi.org/10.1016/j.coastaleng.2015.11.002>
- [29] Deltares (2011). *Delft3D-FLOW – Simulation of Multi- Dimensional Hydrodynamic Flows and Transport Phenomena, Including Sediments*. User Manual Delft3DFLOW, The Netherlands, 690.
- [30] Takagi H, Wu W (2016). Maximum Wind Radius Estimated by the 50 kt Radius: Improvement of Storm Surge Forecasting Over the Western North Pacific. *Natural Hazards and Earth System Sciences*, 16: 705 – 717. <https://doi.org/10.5194/nhess-16-705-2016>
- [31] Egbert G D, Erofeeva S Y (2002). Efficient inverse modeling of barotropic ocean tides. *Journal of Atmospheric and Oceanic Technology*, 19(2): 183 – 204. [https://doi.org/10.1175/15200426\(2002\)019<0183:EIMOBO>2.0.CO;2](https://doi.org/10.1175/15200426(2002)019<0183:EIMOBO>2.0.CO;2)
- [32] Japan Meteorological Agency (2019c). Tidal Observation Data Site (in Japanese). [Available at <http://www.data.jma.go.jp/kaiyou/db/tide/genbo/index.php>]
- [33] Fujii T, Mitsuta Y (1986). Synthesis of a stochastic typhoon model and simulation of typhoon winds. In: *Disaster Prevention Research Institute Annuals*, 29, B-1, 229–239. <https://repository.kulib.kyoto-u.ac.jp/dspace/bitstream/2433/71910/1/a29b1p22.pdf> (In Japanese)

- [34] Bricker J D, Roeber V, Tanaka H (2016). Storm Surge Protection by Tsunami Seawalls in Sendai, Japan. In: Proceedings of 35<sup>th</sup> International Conference on Coastal Engineering, Antalya, Turkey. <https://doi.org/10.9753/icce.v35.management.2>
- [35] Rego J L, Li C (2010). Nonlinear terms in storm surge predictions: Effects of tide and shelf geometry with case study from Hurricane Rita. *Journal of Geophysical Research*, 115: 1–19. <https://doi.org/10.1029/2009JC005285>
- [36] Marsooli R, Lin N (2019). Numerical modeling of historical storm tides and waves and their interactions along the U.S. East and Gulf coasts. *Journal of Geophysical Research: Oceans*, 123: 3844 – 3874. <https://doi.org/10.1029/2017JC013434>
- [37] Japan Meteorological Agency (2019d). Past weather data (in Japanese). [Available at <http://www.data.jma.go.jp/obd/stats/etrn/index.php>]
- [38] Soria J L, Switzer A, Villanoy C L, Fritz H, Bilgera P H T, Cabrera O C, Siringan F P, Maria Y Y S, Ramos R D, Fernandez I G (2016). Repeat storm surge disasters of Typhoon Haiyan and its 1897 predecessor in the Philippines. *Bulletin of the American Meteorological Society*, 97(1): 31 – 48. <https://doi.org/10.1175/BAMS-D-14-00245.1>
- [39] Needham H F, Keim B D (2013). Correlating Storm Surge Heights with Tropical Cyclone Winds at and before Landfall. *Earth Interactions*, 18: 1 – 26. <https://doi.org/10.1175/2013EI000527.1>
- [40] Song H, Kuang C, Gu J, Zou Q, Liang H, Sun X, Ma Z (2020). Nonlinear tide-surge-wave interaction at a shallow coast with large scale sequential harbor constructions. *Estuarine, Coastal and Shelf Science*, 233: 1 – 15. <https://doi.org/10.1016/j.ecss.2019.106543>
- [41] Jelesnianski, C. P. (1972). SPLASH (Special Program to List Amplitudes of Surges from Hurricanes): 1. Landfall storms. In *NOAA Technical Memorandum NWS TDL-46*. Silver Spring, MD: NOAA.
- [42] Thomas A, Dietrich J C, Asher T G, Bell M, Blanton B O, Copeland J H, Cox A T, Dawson C N, Fleming J G, Luettich R A (2019). Influence of Storm Timing and Forward Speed on Tides and Storm Surge during Hurricane Matthew. *Ocean Modelling*, 137: 1–19. <https://doi.org/10.1016/j.ocemod.2019.03.004>
- [43] Islam M R, Takagi H (2019). Statistical significance of tropical cyclone forward speed on storm surge generation: retrospective analysis of best track and tidal data in Japan. *Georisk: Assessment and Management of Risk for Engineered Systems and Geohazards* (Accepted)